

Photometric study of cataclysmic variable ASAS–SN–13cx in active and quite states

Irina Voloshina^{*†}

Sternberg Astronomical Institute, Moscow, Russia

E-mail: voloshina.ira@gmail.com

Tatiana Khruzina

Sternberg Astronomical Institute, Moscow, Russia

E-mail: kts@sai.msu.ru

Qian Shengbang

Yunnan Observatories, Kunming, PRC

E-mail: qsb@ynao.ac.cn

Zhu Liying

Yunnan Observatories, Kunming, PRC

E-mail: zhu@ynao.ac.cn

Stella Kafka

AAVSO, Cambridge, USA

E-mail: skafka@aavso.org

Vladimir Metlov

Sternberg Astronomical Institute, Moscow, Russia

E-mail: vgmetlov@gmail.com

The results of photometric observations of cataclysmic variable ASAS–SN–13cx are presented. CCD observations were taken in August–September 2014 (outburst) and in October–November 2016 (quiescence) using the 50-cm and 60-cm telescopes, more than 1800 images in V and R_c filters. Detailed light curves for the system active and quiescent states are plotted. A “spiral” model is applied to solve for the parameters of ASAS–SN–13cx during the outburst which takes into account the geometric disturbances on the accretion disk surface. We searched for the parameters in quiescence with a “composite” CVs model taking into account an accretion disk with hot spot on the lateral surface geometrically thick outer edge of the disk. The basic parameters of ASAS–SN–13cx are found for the first time including $q = M_1/M_2 = 7.0 \pm 0.2$, $i = 79.9 \div 80.1^\circ$, $a_0 = 0.821(1)R_\odot$, radiuses $R_1 = 0.0102(4)R_\odot$, $R_2 = 0.194(3)R_\odot$ and temperatures of the components $T_1 = 12500 \pm 280$ K, $T_2 = 2550 \pm 400$ K. These parameters correspond to M4–9 V spectrum of the secondary. The mass of the accretion disk approximately doubles during quiescence on a time scale of about 400 orbital periods. The classification of ASAS-SN-13cx as a SU UMa dwarf nova is confirmed.

The Golden Age of Cataclysmic Variables and Related Objects IV

11-16 September, 2017

Palermo, Italy

*Speaker.

†This study has been supported via RFBR grant No17-52-53200

1. About ASAS-SN-13cx system

Transient ASAS-SN-13cx (Andromeda constellation), $V = 15.^m47$ with coordinates $02^h02^m22.4^s$, $+42^\circ42'14.''2$, was discovered in course of realization of ASAS-SN project on September 14, 2013. The other names of this object: CMC15 J000222.3+424213, CSS J000222.4+424213, GSC2.3 NBGH007685, USN-A2.0 1275-00025147, USN-B1.0 1327-0001011. 6 outbursts were detected during Catalina Real-time Transient Survey. CRTS data supposed that the average super-outburst cycle could be $\sim 350^d$ or half of it. International campaign, organized in August 2014 during outburst [1] permits to suggest that it is probable eclipsing cataclysmic variable.

2. Observations

Our observations of ASAS-SN-13cx were done with the help of two telescopes of Sternberg Astronomical Institute in Crimea in 2014 (during the outburst) and in 2016 (during quiescence). Both telescopes are shown on Fig. 1 60-cm telescope equipped with Apogee 47 detector (field size 1024×1024 pixels, 1 pixel = 13 mkm). 50-cm telescope equipped with an Apogee Alta U8300 detector (field 3326×2504 pixels, 1 pixel = 5.41 mkm). Maximum of efficiency is 60% at $\lambda 5800 \div 6600\text{\AA}$ and 30% — at $\lambda 4000\text{\AA}$. Duration of observational sets depended from sky conditions and usually lasted from 4 to 7 hours (to cover 2–3 orbital cycles). We used the local standard 133 from the list of AAVSO standards with coordinates $\alpha = 0^h02^m06^s.71$ and $\delta = +42^\circ41'50.1''$ ($V = 13.^m320$, $R_c = 12.^m922$). Our data are accurate to $0.02 - 0.06^m$. The details of our observations are presented in Table 1.



Figure 1: 60-cm telescope with Apogee-47 CCD (left). 50-cm telescope with an Apogee Alta U8300 (right)

Observational light curves of ASAS-SN-13cx during the outburst were obtained at the beginning of September 2014 (the outburst maximum was observed on August 31, 2014).

A new short-term brightness increase (outburst) of ASAS-SN-13cx was detected on October 5, 2016 with $V = 15.^m2$ [2]. The V - band out-of-eclipse brightness of the object was $V = 16.^m5$ and $V = 18.^m2$ on October 9 and 14, respectively. By the beginning of our observations in the R_c

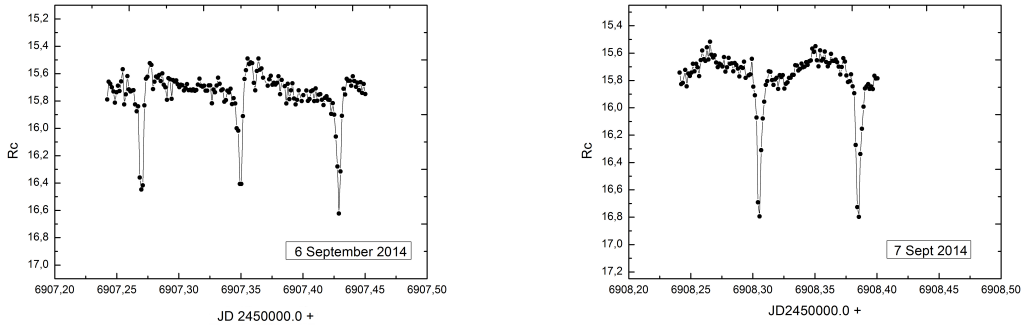


Figure 2: Individual light curves of ASAS–SN–13cx obtained with 50 cm telescope during outburst of 2014

filter (October 18, 2016), the out-of-eclipse brightness of ASAS–SN–13cx had already returned to its normal, post-outburst level, $R_c = 18^m$. In our observations of November 4, 2016 (JD 245 6697) a short-term brightness increase by $1^m.5$ was detected; the flat shape of the out-of-eclipse part of the light curve indicated that the event was due to a considerable increase in the light flux coming from the disk. These observations of ASAS–SN–13cx covered about 440 orbital cycles (8 light curves) during a quiescent stage.

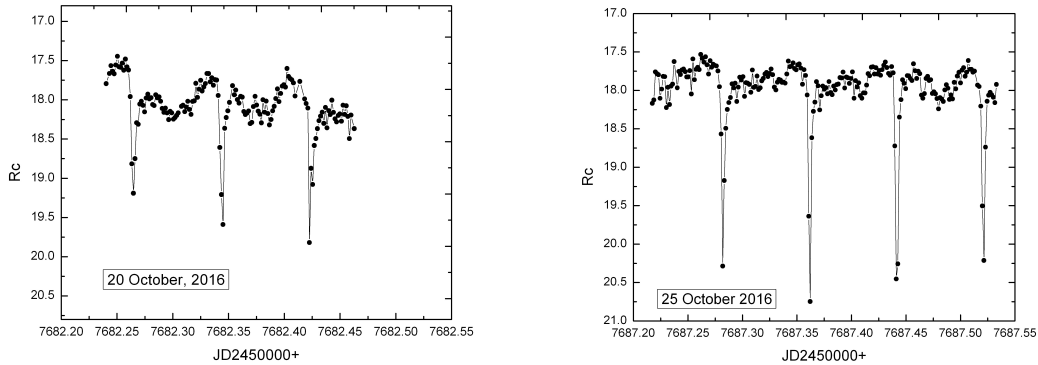


Figure 3: Observational light curves of ASAS–SN–13cx during quiescence obtained with 60-cm telescope

The details of our observations one can find in Table 1.

For the completeness of our analysis we also used AAVSO light curves obtained in the white light C and V band during outburst in September 2014 (12 curves at all). Some of these curves are shown in Fig. 4. The overall light curve of ASAS–SN–13cx for superoutburst of 2014 constructed by AAVSO data is shown on the Fig. 5.

Eight observing runs in 2016 (quiescence, October 18—November 22) were obtained with the 60-cm Zeiss-600 (Zeiss-2) telescope and five of the 13 observing runs were obtained with the 50-cm AZT-5 telescope (September 5–7, 2014 and October 18, 2016): one of these was in the V band and four in the R_c filter. To get a uniform data set for our analysis, we observed ASAS–SN–13cx simultaneously with the two telescopes on single night. A comparison of the resulting light curves

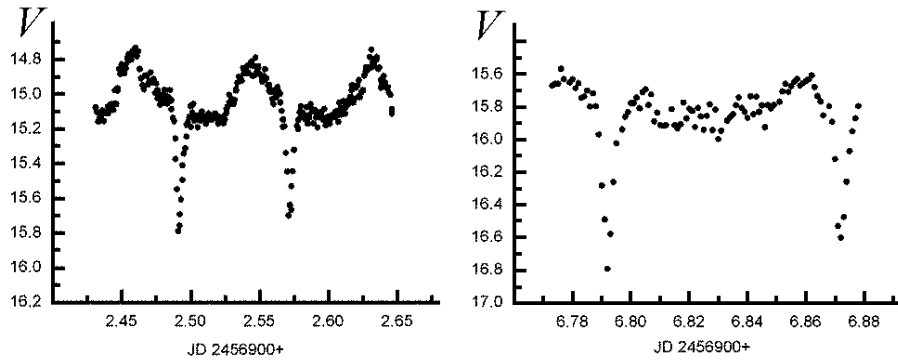


Figure 4: Individual light curves of ASAS-SN-13cx in V band which were obtained by AAVSO observers

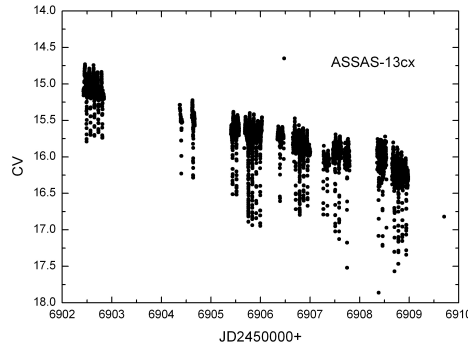


Figure 5: The overall light curve of ASAS-SN-13cx by AAVSO observations in outburst of 2014

indicated that, in order to reduce the observations performed with the 50-cm telescope (Rc50) to the 60-cm instrumental system (Rc60), a magnitude correction

$$Rc60 = Rc50 - 0.05^m$$

is needed. As an example, Fig. 6 displays the light curves of ASAS-SN-13cx obtained with the two telescopes on October 18, 2016: the red circles show data from the 60-cm telescope and the black circles data from the 50-cm telescope. This figure clearly shows that the shifted curves are practically identical in their overlapping parts. All our subsequent computations were performed for the Zeiss-600 instrumental system to obtain a homogeneous dataset.

The light curves we obtained were used to determine the parameters of the system and to study the character of their variations in different activity stages. Consideration of all light curves of ASAS-SN-13cx evidences that the shape of obtained light curves and the depth of minimums even for the same state are different, therefore the light curve of ASAS-SN-13cx for every night was analysed separately.

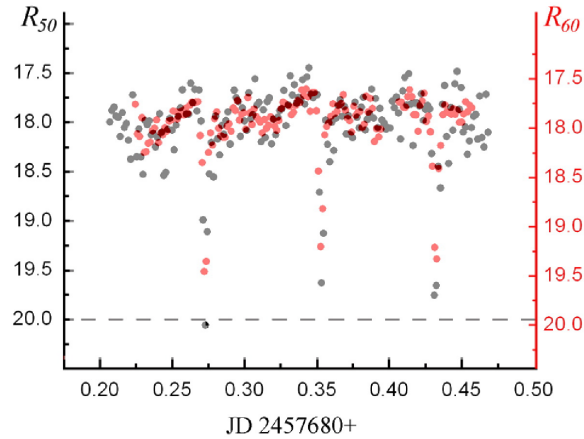


Figure 6: Comparison of photometric observations of ASAS–SN–13cx obtained simultaneously on 18 October 2016 (JD 7680) with the 60 cm (red points, R60) and 50 cm (black points, R50) telescopes in order to reveal instrumental differences.

3. Superhumps period search

We applied the standard procedure used when searching for superhump periods. For each dataset, we determined the mean out-of-eclipse brightness (the eclipses of the program binary are at phases $\Delta\phi \sim 0.90 \div 1.13$, we took a slightly broader range of eclipse phases) and calculated the deviations of the observations from the derived mean, ΔR_c . We used the combined observations to derive a Fourier spectrum in order to independently determine the superhump period for a given part of the descending branch of the outburst. Period search was done with step 0.00002. Obtained in this paper value of superhumps period $P_{sh} = 0^d.08301(12)$ is in good agreement with P_{sh} for the stage B from [3], — $P(sh1) = 0^d.083098(42)$ (see Fig. 7 below).

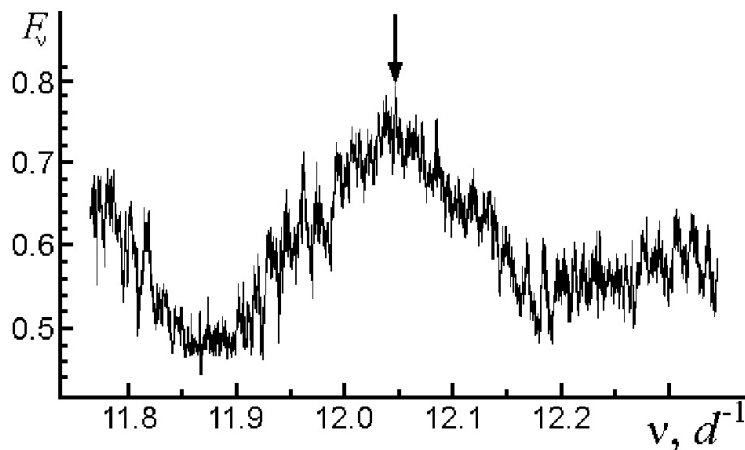


Figure 7: Part of the Fourier spectrum for the region of the superhump period. The arrow marks the maximum of the frequency distribution corresponding to the period $P_{sh} = 0.0830101^d$.

Table 1: Journal of observations

Date	set start–set end	telescope	band	resolution	N
05.09.2014	6906.405-6906.490	50 cm	V	60 s	108
05.09.2014	6906.260-6906.403	50 cm	r_c	60 s	179
06.09.2014	6907.242-6907.450	50 cm	r_c	100 s	162
07.09.2014	6908.241-6908.400	50 cm	r_c	100 s	127
17.10.2015	7313.462-7313.576	50 cm	r_c	90 s	98
19.10.2015	7315.368-7315.501	50 cm	r_c	120 s	89
18.10.2016	7680.224-7680.457	60 cm	R_c	120 s	154
18.10.2016	7680.207-7680.468	50 cm	r_c	120 s	180
20.10.2016	7682.249-7682.463	60 cm	R_c	120 s	148
20.10.2016	7682.187-7682.455	50 cm	V	120 s	176
25.10.2016	7687.217-7687.533	60 cm	R_c	120 s	219
04.11.2016	7697.188-7697.422	60 cm	R_c	60 s	299

4. Models

We used the following model for fitting of light curves SU UMa system: a normal star (a red dwarf) fills its Roche lobe and the other component — a spherical star (white dwarf), is surrounded by an elliptical geometrically thick accretion disk. Our analysis clearly show that obtained light curves of our star differ by shape and minima depths, therefore every curve considered separately. Different models were used for both states:

1. A standard, “composite” model taking into account the presence of a hot line near the lateral surface of the disk and a hot spot on the disk, on the leeward side of the stream [4]. We used this model when analysing the light curves in quiescence, assuming there were no geometric perturbations of the inner surface of the disk in this state.
2. A “spiral” model that schematically takes into account the presence of spiral waves in the disk, with the height of the wave crests dependent on the z coordinate of a point on the disk’s surface, so that the crest height is largest near the disk edge and rapidly decreases towards the white dwarf [5].

5. Our results

We found the system parameters providing the shape of the synthetic light curve most closely matching the observed one applying the Nelder-Mead method [6]. The synthetic ASAS-SN-13cx light curves computed with these parameters are shown in the Fig. 8, Fig. 9 below.

Results of our determination of the ASAS-SN-13cx system parameters during outburst (for JD 906 and JD 907) are shown on the Fig. 8. The diagram shows the observations (points in left panel, points with corresponding error bars on the mean curves (in the middle) and the synthetic light curves (solid coloured curves in the right), folded with the orbital period. The right panels show the contributions from the system components to the combined flux (in conditional units):

(1) the white dwarfs and (2) the red dwarfs, (3) the accretion disk with the spiral structure on its surface, and (4) the hot line. The figure shows the contributions of the system components to the combined flux in conditional units. On all dates, the main contribution to the combined flux is made by the accretion disk; this contribution decreases with time, being 20.2 and 17 conditional units on JD 906 and 907 respectively.

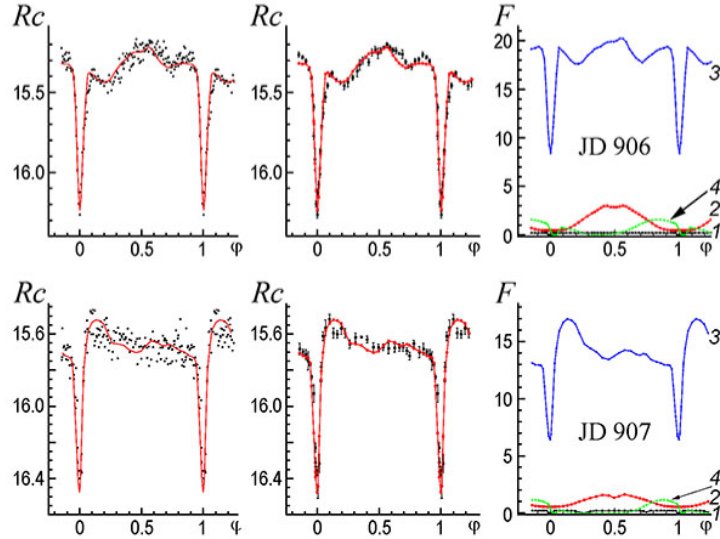


Figure 8: Left panels—observations (points), theoretical light curves (red curves); panels in the middle – the same for mean light curves. Right panels—contribution of various components to the total flux: 1 – white dwarf; 2 – red dwarf; 3 – disk with spirals; 4 – hot line. Disk gives the highest contribution every date, contribution of hot line is small, less than for red dwarf. Contribution of red dwarf on JD 907 is lower than for other dates. Out-of-eclipse flux $R_c \sim 15.^m5$.

Some results of determining the ASAS–SN–13cx system parameters in quiescence are shown on the Fig. 9. Left panels: the mean light curves (points with error bars) and synthetic light curve. The inserts display the unaveraged observations and the synthetic light curves near orbital phases $\Delta\phi = 0.9 \div 1.1$. The marks along the vertical axes for the inserts are the same as those for the full light curves. Right panels: contributions to the combined flux (in conditional units) from the system components: (1) the white dwarf, (2) red dwarf, (3) accretion disk with the hot spot on its lateral surface, and (4) hot line. The quiescence light curves have variable amplitudes as well as shapes, indicating instability of the system at this stage. Bearing in mind the considerable flickering in the observations, there is satisfactory agreement between the theoretical and observed light curves. The flickering is considerably lower in the primary minimum than in out-of-eclipse parts of the light curves.

Fig. 10 shows the time variations of several of the system parameters (plotted as a function of the number of orbital cycles N since the beginning of our observations): its R_c brightness, temperature of the secondary T_2 , and characteristics of the accretion disk — its semi-major axis a , the temperature at its outer edge T_{out} and in the boundary layer T_{in} , the half-thickness of the outer edge of the disk $0.5\beta_d$, and the index α_g determining the radial distribution of the temperature. We show the parameters of the system during the descending branch of the outburst to the left of the

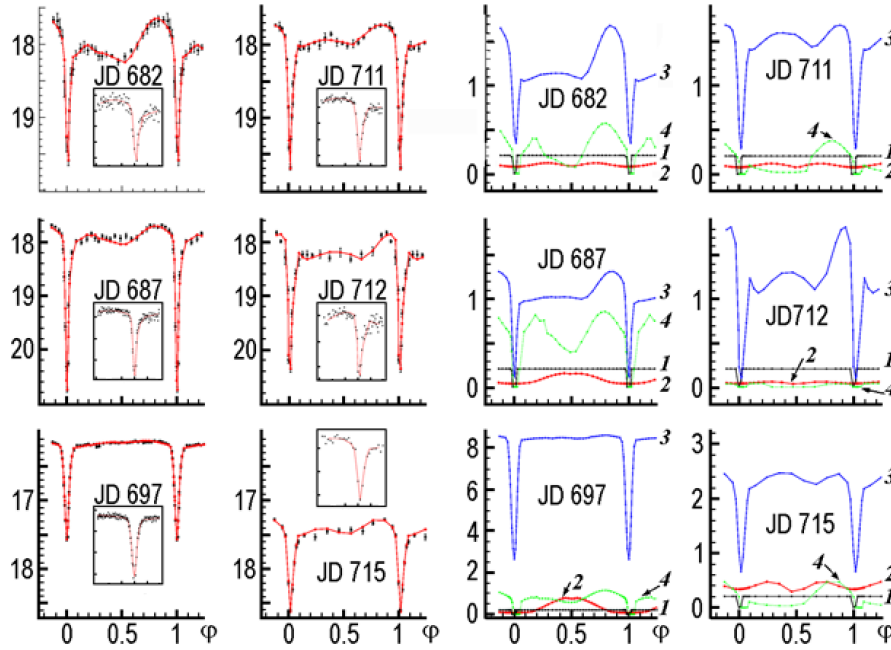


Figure 9: The left panels — mean light curves and theoretical curves (red solid line). Windows show un-averaged observations and theoretical light curves in a range $0.9 \div -1.1$. The right panels show contribution of the system components to the total flux: 1 – white dwarf; 2 – red dwarf; 3 – accretion disk with hot spot; 4 – hot line. Contribution of accretion disk is the highest one on JD 697 (8 cond.un.). Out-of-eclipse flux is unstable, but on average $R_c \sim (17.4 \div 17.6)^m$.

vertical dashed line and the parameters in quiescence to the right of this line.

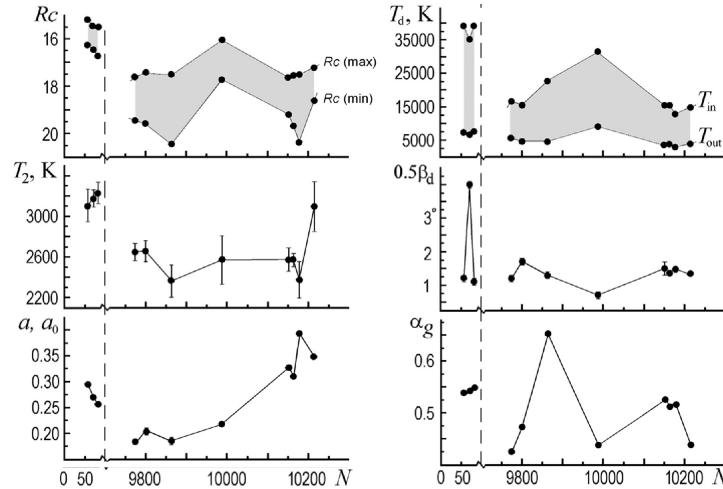


Figure 10: Dependence on the orbital cycle number N of the maximum and minimum flux from the system in the R_c filter (the variation amplitude is shown by grey shading), the effective temperature of the secondary T_2 , the semi-major axis a of the elliptical accretion disk (on the left panels), the temperature in the disk boundary layer T_{in} and at the outer edge of the disk T_{out} (the variation amplitude is shown by grey shading), the half-thickness of the disk's outer edge (in degrees) $0.5\beta_d$, and the index α_g .

The Table 2 shows some of the obtained parameters of accretion disk and hot line and how they changes from quiet state to outburst (by data in R band). T_{in} temperature of inner regions of the disk, $T(lw)$ — the temperature of leeward side of gaseous stream, $T(ww)$ — the temperature of windward side of gaseous stream, β_d , — thickness of the outer edge of accretion disk

Table 2: Variations of accretion disk and hot line parameters in R band

Parameter	Inactive state, (15 nights)	Active state (2 nights)
R_d, a_0	0.184–0.393	0.256–0.295
e	0.02–0.10	0.02–0.06
$0.5\beta_d, ^\circ$	0.7–1.7	1.1–4.0
T_{in}, K	12900–31300	35000–39300
	0.4–0.65	0.54–0.55
$T(ww), K$	8700–16200	26700–36100
$T(lw), K$	11900–16300	9400–14300

6. Conclusions

We have presented our new photometric observations in R_c band of the eclipsing cataclysmic variable ASAS–SN–13cx, an SU UMa dwarf nova, during the descending branch following the outburst maximum in September 2014 and in a quiescent period in October–November 2016. We have performed a detailed analysis of the available observations. The light curves we obtained are in good agreement with observations from the AAVSO database.

From our analysis we could conclude the following:

- The basic system parameters are determined for the first time, — $q = M_1/M_2 = 7.0 \pm 0.2$, $i = 79.94 \pm 0.24^\circ$, $a_0 = 0.821(1)R_\odot$, $R_1 = 0.0124(5)a_0 = 0.0102(4)R_\odot$, $R_2 = 0.236(4)a_0 = 0.194(3)R_\odot$, $T_1 = 12\,500 \pm 280$ K, $T_2 = 2550 \pm 400$ K;
- These parameters correspond to M4–9 V spectrum of the secondary;
- The radius of the accretion disk approximately doubles during quiescence on a time scale of about 400 orbital periods. It evidence of storage material in the disk In active state radius of accretion disk go down from $\sim 0.3a_0$ to $0.2a_0$;
- The classification of ASAS–SN–13cx as a SU UMa dwarf nova is confirmed: short $P_{orb} = 0^d.079650075 = 1^h.9116$ (less than 2^h), existence of superhumps on the light curve of ASAS–SN–13cx, which moved with the period $P_{sh} = 0^d.08301(12)$, value of superhump period excess $\varepsilon = (P_{sh} - P_{orb})/P_{orb} = 0.042(2)$ and $q \sim 7$, – indicated to ASAS–SN–13cx classification as SU UMa star;
- There is no any dependence between out-of-eclipse flux R_c and depth of eclipse minimum.

Main conclusion of our study: *main source of variations of ASAS-SN-13cx light curves is alternations of accretion disk structure and parameters of the system.*

Acknowledgements. Authors are very grateful to Dr. Valerian Sementsov for useful discussion on obtained results.

References

- [1] E. de Miguel and T. Kato, VSNET-alert, No 17684 (2014).
- [2] T.Kato, VSNET-alert, No 20215 (2016).
- [3] T. Kato, F.-J. Hamsch, P. A. Dubovsky, I. Kudzej, et al., Astron. Soc. Jpn. **67**, 105 (2015).
- [4] T.S. Khruzina, Astron. Rep. **55**, 425 (2011)
- [5] T.S. Khruzina, Astron. Rep. **49**, 783 (2005)
- [6] D. Himmelblau, Applied Nonlinear Programming (McGraw-Hill, New York, 1972).